Guzman, B. G. & Jimenez, V. P. G. (2017). DCO-OFDM Signals with Derated Power for Visible Light Communications Using an Optimized Adaptive Network-Based Fuzzy Inference System. *IEEE Transactions on Communications*, 65(10), pp. 4371-4381.

DOI: 10.1109/tcomm.2017.2722477

DCO-OFDM Signals with Derated Power for Visible Light Communications Using an Optimized Adaptive Network-Based Fuzzy Inference System (ANFIS)

Borja Genovés Guzmán, *Student Member, IEEE,* and Víctor P. Gil Jiménez, *Senior Member, IEEE*

***Abstract*—Direct Current-biased Optical Orthogonal Frequency Division Multiplexing (DCO-OFDM) signals used in Visible Light Communications (VLC) suffer from high Peak-to-Average-Power Ratio (PAPR) or Cubic Metric (CM). It strongly degrades the performance due to the great back-off necessary to avoid the clipping effect in the Light-Emitting Diode (LED). Thus, PAPR and CM reduction techniques become crucial to improve the system performance. In this paper, an Adaptive Network-based Fuzzy Inference System (ANFIS) is used to obtain efficient DCO-OFDM signals with a low power envelope profile. Firstly, signals specially designed for DCO-OFDM with very low CM, as the ones obtained from the Raw Cubic Metric - Active Constellation Extension (RCM-ACE) method, are used to train the fuzzy systems in time and frequency domains. Secondly, after the off-line training, the ANFIS can generate a real-valued signal in a one-shot way with 8.9 dB of RCM reduction from the original real-valued signal, which involves a gain in the Input Power Back-Off (IBO) larger than 2.8 dB, an Illumination-to-Communication conversion Efficiency (ICE) gain of more than 35 % and considerable improvements in Bit Error Rate (BER).**

***Index Terms*—Adaptive Network-based Fuzzy Inference System (ANFIS), Cubic Metric (CM), Direct Current-biased Optical Orthogonal Frequency Division Multiplexing (DCO-OFDM), Peak-to-Average-Power Ratio (PAPR), Visible Light Communication (VLC).**

I. Introduction

NOWADAYS there is an increasing demand of high speed data rate services in wireless communications. Technologies such as the Fifth Mobile Generation (5G) [1] promise binary data rate above Gbps. However, inter-cell interference, especially in heterogeneous networks (HetNets) [2], and spectrum limitations make it complicated to achieve that performance. In these scenarios, Visible Light Communication (VLC) appears as a solution.

Now that VLC is on the market [3], there are standards [4] and multiple proposals to increase reliability [5], VLC starts to be considered as a candidate [1] to supply these services and satisfy the user demands. Complex and efficient modulations schemes have been adapted to optics due to the need of achieving higher data rate and dealing with the Intersymbol Interference (ISI), namely: Direct Current-biased Optical Orthogonal Frequency Division Multiplexing (DCO-OFDM) [6], Asymmetrically Clipped Optical OFDM (ACO-OFDM) [7] and Flip-OFDM [8]. All those alternatives provide real-valued and unipolar signals because of the Intensity Modulation/Direct Detection (IM/DD) techniques required in VLC. Owing to the good spectral efficiency of DCO-OFDM compared to the previous methods [9] and its DC configurable value used for illumination, we will focus on DCO-OFDM systems.

OFDM has the disadvantage of suffering from the high Peak-to-Average Power Ratio (PAPR), and for this reason large power back-offs are needed at the Light-Emitting Diodes (LEDs). The back-off is necessary to make the signal work in the linear zone and then, to avoid signal degradation, similarly to the back-off at the High Power Amplifiers (HPA) in radio frequency systems. The larger the PAPR, the larger the back-off is needed, and, as a result, the signal is more compressed and inefficient. In that case, the signal does not take advantage of the LED's linear range and its performance is reduced. If the PAPR is reduced, the needed back-off will be lower and the signal will work properly in the linear range with higher efficiency. This is, in systems where multicarrier modulations are used, PAPR reduction techniques are essential.

PAPR reduction techniques were proposed as a solution to this problem in radiofrequency systems [10]. However, the literature demonstrates that the Cubic Metric (CM) is a more effective indicator of the power derating factor because it uses higher order statistics [11], whereas PAPR only considers the maximum signal peak. A first proposal to reduce the CM in DCO-OFDM VLC systems was published in [12]. It adapts the well-known Active Constellation Extension (ACE) algorithm to optical signals, and proposes a new ACE technique (denoted as RCM-ACE from this point forward) by adding two modifications to the traditional one: the optimization by means of CM instead of PAPR, and the change of the clipping stage for a two-valued signal ($[+V_{clip}\ -V_{clip}]$). Although it yields good results, it has limited flexibility in the saturation process, causing unbalanced constellations because of saturated symbols.

Due to the flexibility of an Adaptive Network-based Fuzzy Inference System (ANFIS), its capacity of being trained and reducing its complexity [13], this paper proposes a CM reduction technique using an architecture based on ANFIS. These fuzzy networks were already applied to radiofrequency systems in [14] to reduce the CM in OFDM signals, but the

The authors are with the Signal Theory and Communications Department at Universidad Carlos III de Madrid, Leganés (Madrid), 28911 Spain (e-mail: bgenoves@tsc.uc3m.es; vgil@tsc.uc3m.es).

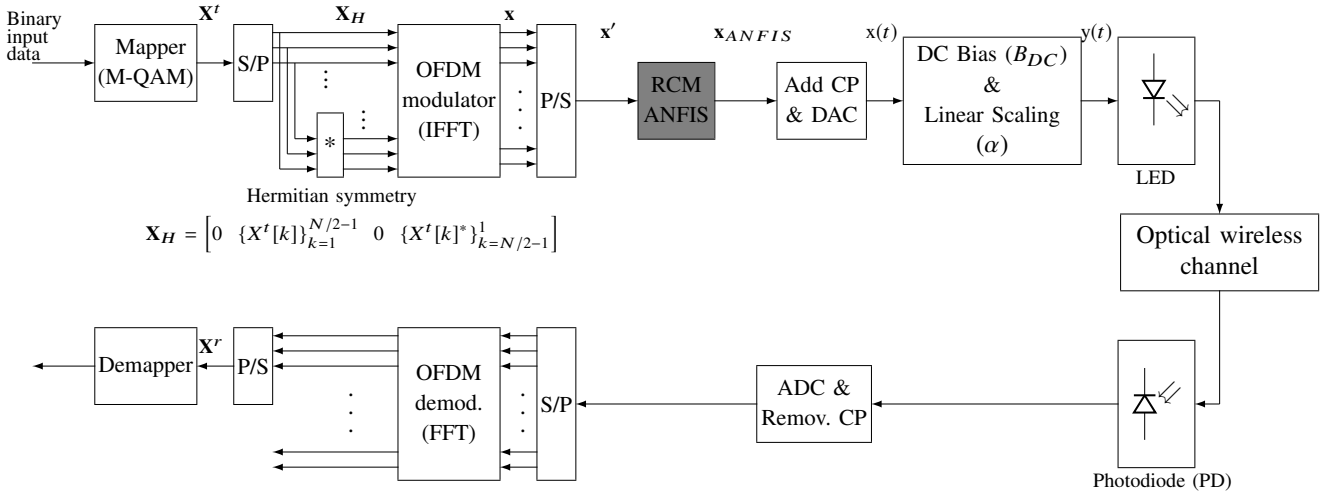

Fig. 1: DCO-OFDM system model with the proposed RCM-ANFIS in VLC.

inherent different nature of RF signals in comparison to optical ones makes that scheme invalid to be used in DCO-OFDM.

This proposal uses two stages, whose ANFIS are trained with signals resulting from the RCM- ACE technique. The first ANFIS works with signals in the time domain (time-domain stage), whereas the second ANFIS set works with signals in the frequency domain (frequency-domain stage). The signals used to train the time-domain stage have a soft saturation. Afterwards, the output will go over the frequency-domain stage, which is trained with severely saturated signals in order to have an energy efficient output.

This paper is organized as follows: the system model, metrics and figures of merit used in the paper are introduced in Section II; the neuro fuzzy systems used in the proposal are explained in Section III; then, the proposed solution is described in Section IV, and the results are presented and discussed in Section V. Finally, conclusions are drawn in Section VI.

Note: The following notation will be used throughout the paper: boldface symbols will denote vectors whereas normal-face, scalars; time-domain signals will be written in small-case letters, and frequency-domain signals will be used in capitalized letters.

II. System Model

In a multicarrier system, the time-domain complex baseband transmitted signal $\mathbf{x}$ for an OFDM symbol is defined as

$$\mathbf{x} = \{x[0] \cdots x[N-1]\}^T = \frac{1}{\sqrt{N}} \sum_{k=0}^{N-1} X_H[k] e^{\frac{j2\pi kn}{N}} \quad (1)$$

where N is the number of subcarriers and $X_H[k]$ are the complex modulated base-band symbols in frequency domain on the k-th subcarrier. In DCO-OFDM, subcarriers 1 and $N/2$ are zero-valued. In addition, the last N/2-1 subcarriers are conformed by the Hermitian symmetry of the subcarriers from 1 to $N/2-1$ to guarantee a time-domain real-valued signal. Thus, $\mathbf{X}_H = \left[0 \;\; \{X^t[k]\}_{k=1}^{N/2-1} \;\; 0 \;\; \{X^t[k]^*\}_{k=N/2-1}^{1}\right]$, where $\mathbf{X}^t$ are the transmitted symbols.

The diagram of the DCO-OFDM system used in this paper is shown on Fig. 1. Once the symbols of a M-QAM constellation have been generated, an Inverse Fast Fourier Transform (IFFT) of N points is applied after having carried out a Hermitian symmetry. The signal is transformed from parallel to serial, and feeds the grey box which is the proposed ANFIS method. ANFIS is based on fuzzy rules (heuristics) [13] [15] that are here optimized to reduce the CM of the input signal. After that, a Cyclic Prefix (CP) is added, and the bipolar real-valued signal in the time domain ($x(t)$) is obtained by means of a Digital to Analog Converter (DAC). The unipolar and well suited to the LED transfer function forward signal ($y(t)$) results from adding the DC bias and a linear scaling. On the receiver side, a photodiode detects the optical intensity and turns it into the amplitude of an electrical signal. Binary data are obtained with the reversed transmitter procedure. Note that ANFIS is only necessary on the transmitter side and no side information is needed either. The reason is that ANFIS changes the signal properties before the transmission, which involves that IQ symbols are distanced from the decision borders always within the allowable region. Thus, it does not affect the Demapper procedure at the receiver because the allowable region does not compromise the Bit Error Rate (BER) or the symbol demapping [10].

Although channel equalisation is out of the scope of this work, note that pilot symbols used for channel estimation purposes must not be modified by any PAPR or CM reduction technique on the transmitter side [16]. Besides, since frequency-domain symbols are distanced from the decision borders, they keep offering benefit even when a channel equalization is carried out.

A. Metrics

In order to evaluate the performance of the proposed scheme in terms of envelope variations, the CM is used in contrast

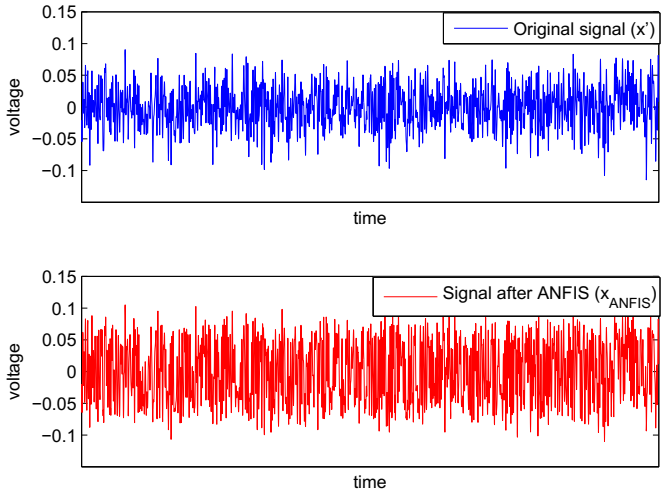

Fig. 2: Effect in the time domain of RCM-ANFIS.

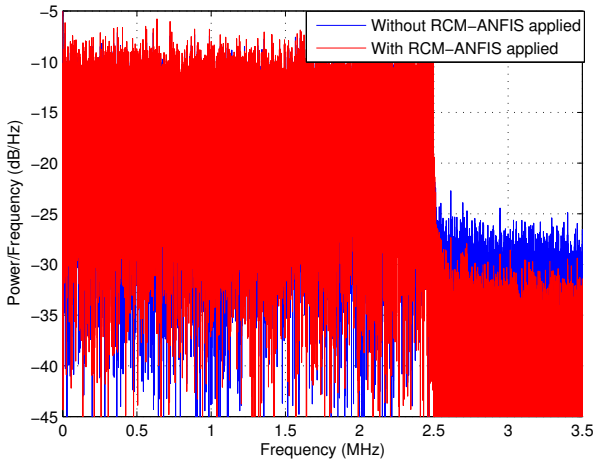

Fig. 3: Power density spectrum of the signal in the output of the LED when it is not modified, and when its CM is reduced by RCM-ANFIS.

to the classic PAPR metric. The CM [11] uses higher order statistics and thus it is better for evaluating the distortion produced by the non-linear transfer function of a HPA or an LED [12]. It is defined as

$$CM(x(t))|_{dB} = \frac{RCM(x(t))|_{dB} - RCM_{ref}}{K}, \quad (2)$$

where RCM is the Raw Cubic Metric and RCM_{ref} and K are constant values depending on the communication system. Following the idea in [12], the focus will be to reduce the RCM as much as possible without increasing the signal energy

$$RCM(x(t))|_{dB} = 20 \cdot log\left(rms\left[\left(\frac{|x(t)|}{rms[x(t)]}\right)^3\right]\right), \quad (3)$$

where rms stands for the root mean square within a time-domain OFDM symbol.

The RCM must be evaluated before the linear scaling and biasing operation in order not to affect the metric and distort it. After these two operations, the real signal might be expressed as

$$y(t) = \alpha \cdot x(t) + B_{DC}. \quad (4)$$

The real value B_{DC} is used for guaranteeing a unipolar signal, whereas the real value α is used for scaling $x(t)$ within the Dynamic Range (DR) of the LED defined as

$$DR = V_{SAT} - V_{TOV}, \quad (5)$$

being V_{TOV} the turn-on voltage and V_{SAT} the saturation input voltage. By using an ideal linear LED input-output characteristic [12], these parameters give rise to others, such as the average optical power (O_{AVG}), associated with the input average voltage (V_{AVG}), and the saturation output optical power (O_{SAT}), associated with V_{SAT}. Indeed, O_{AVG} is also defined as the required illumination level, and establishes the B_{DC} that is the mean value of $y(t)$. As introduced in [12], the B_{DC} and α parameters determine the Biasing Ratio (BR) and the Input power Back-Off (IBO) [17], defined as

$$BR = (B_{DC} - V_{TOV})/DR, \quad (6)$$

and

$$IBO = DR^2/(\alpha^2 \cdot \sigma_x^2), \quad (7)$$

being σ_x^2 the variance of $x(t)$.

The scale factor α must be chosen in such a way that the system works properly within the dynamic range of the LED. A low value of α implies a low variance (σ_y^2) which means a bad use of the dynamic range of the LED, whereas a high value of α can result in a clipping effect in the optical signal. Thus, scale factor α controls the necessary IBO defined in eq. (7). The IBO represents a decrease in the maximum output optical power level in order to guarantee that the entire signal is within the linear region of the LED.

The lower the IBO, the higher the power of the signal at the input of the LED, but at the same time the signal distortion can increase due to the clipping effect.

Fig. 2 and Fig. 3 represent the comparison of $\mathbf{x}'$ and $\mathbf{x}_{ANFIS}$ (See Fig. 1) and its influence in the power spectral density at the LED ouput, respectively. In the time domain $\mathbf{x}_{ANFIS}$ has a larger variance than $\mathbf{x}'$, and as a result, the metric IBO showed in eq. (7) is lower, assuming the same linear scaling parameter (α) because both signals have the same amplitude. Thus, working with $\mathbf{x}_{ANFIS}$ involves taking better advantage of the dynamic range of the LED, and then, providing better results. Note in Fig. 3 that there is out-of-band energy when the CM is not reduced. This image represents the power density spectrum of the signal at the LED output, once it has gone through the RCM-ANFIS.

B. Figures of merit

Two metrics are used to evaluate the performance of this proposal.

1) Error Vector Magnitude (EVM). It detects the signal distortions, and is defined as

$$EVM = \sqrt{\sum_{p=0}^{P-1} |X^r[p] - X^t[p]|^2 / \sum_{p=0}^{P-1} |X^t[p]|^2}, \quad (8)$$

where P is the total number of symbols, and $X^r[p]$ and $X^t[p]$ are the p^{th} received and transmitted constellation points, respectively.

2) Illumination-to-Communication conversion Efficiency (ICE) to study the VLC system efficiency. Defined as [17]

$$ICE = D_o/O_{AVG} = D_i/(V_{AVG} - V_{TOV}), \quad (9)$$

being D_o the standard deviation of the output intensity, and D_i the standard deviation of the input electrical signal given by $y(t)$. [18] shows the importance of ICE to quantify the VLC performance, where illumination and communication take place simultaneously. The ICE is closely related to a parameter called Brightness Factor (BF) [17], formulated as

$$BF = O_{AVG}/O_{SAT} = (V_{AVG} - V_{TOV})/DR. \quad (10)$$

Since VLC systems illuminate and transmit information at once, we need to consider the illumination level as well. It is given by the aforementioned parameter O_{AVG}, but it is also related to the BF as it can be verified in eq. (10).

The parameter BF is theoretically between 0 and 1, but in a practical scenario it must be lower than a BF_{max} value, which is restricted by the maximum permissible DC voltage of the LED. The communication capacity is related to the illumination using the ICE parameter. Comparing eq. (9) and eq. (10), the higher the ICE, the lower the brightness factor or illumination level is and thus, the transmission capacity. Therefore, a tradeoff between ICE and BF must be found.

III. Neuro-fuzzy System

In this paper, neuro-fuzzy systems are applied to reduce the RCM in DCO-OFDM for VLC systems and, therefore, also the CM. The proposal offers the chance of training in time and frequency domains. The characteristics of the desired signal for each domain will be improved (see Section IV).

A Fuzzy `if then` rule is an expression as `IF` Φ THEN Ψ, where Φ and Ψ are labels of fuzzy sets. This fuzzy form was proposed by Takagi and Sugeno in [13], and it has a great capacity to learn how to approximate non-linear functions. Here, the typical fuzzy rule will be utilized in a Sugeno's fuzzy model [15], whose format, considering two inputs and one output (for simplicity), is

$$\textbf{If } \phi \textit{ is } \Phi \textit{ and } \psi \textit{ is } \Psi \textbf{ then } z = f(\phi, \psi), \quad (11)$$

where Φ and Ψ are the fuzzy sets and $z = f(\phi, \psi)$ is a defined function.

An adaptive network has multiple applications because there are barely restrictions on the node functions. Structurally the only limitation of the network configuration is that it should be of the feedforward type [13]. The ANFIS is an adaptive-network-based fuzzy inference system, *i.e.*, it is an adaptive network whose functionality is equivalent to a fuzzy inference system. In our application, the signal is received and the goal is to obtain an output with the desired characteristics. It is obtained with fuzzy rules of the type `if then`. The main drawback of the fuzzy rules is the need of expert knowledge or instructions to define them, and thus, knowing the parameters of the f functions turns into a hard task. However, fuzzy rules and an adaptive network can be combined in such a way that those parameters can be trained in that adaptive network. The system becomes very useful because the disadvantages of using fuzzy rules are overcome with the advantages of using neural networks. This structure results in a hybrid network which combines both a fuzzy system and a neural network. It is denoted ANFIS, and it was proposed in [13].

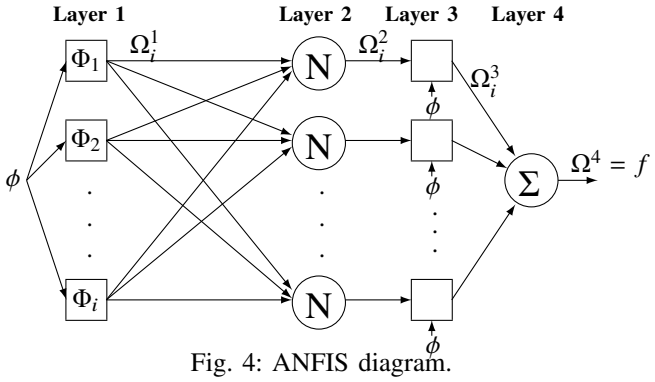

Fig. 4: ANFIS diagram.

A. Proposed Neuro-fuzzy System

The implementation of the proposed ANFIS is based on different layers where their corresponding nodes compute an operation. This procedure can be followed in Fig. 4. Note that only one input exists for our problem.

At layer 1: Membership functions with Gaussian shape are considered, and they are defined as

$$\Omega_i^1 = \mu_{\Phi_i}(\phi) = exp(-\frac{(\phi - c_i)^2}{a_i}) \quad (12)$$

where Φ_i is the linguistic label (small, large, etc.) associated with the i^{th} node, and c_i and a_i are the premise parameters. The maximum of Ω_i^1 is equal to 1 and the minimum equals 0. Since only one input exists in our design, Ω_i^1 matches the firing strength: $\Omega_i^1 = \omega_i$.

At layer 2: The i^{th} node calculates the ratio of the i^{th} rule's firing strength, called normalized firing strengths

$$\Omega_i^2 = \frac{\omega_i}{\sum_i \omega_i} = \overline{\omega}_i. \quad (13)$$

At layer 3: Each node computes its contribution to the overall output as

$$\Omega_i^3 = \overline{\omega}_i f_i = \overline{\omega}_i(p_i\phi + r_i), \quad (14)$$

where p_i and r_i are the consequent parameters.

At layer 4: The overall output is calculated as the summation of all incoming signals:

$$\Omega^4 = \sum_i \overline{\omega}_i f_i = \frac{\sum_i \omega_i f_i}{\sum_i \omega_i}. \quad (15)$$

The first-order Sugeno fuzzy inference system designed i this work contains i `if then` rules

$$\text{If } \phi \, is \, \Phi_i \text{ then } f_i = p_i\phi + r_i$$

and given the premise parameters (c_i and a_i), the overall outp can be expressed as a linear combination of the consequ parameters (p_i and r_i)

$$\Omega^4 = f = \frac{\sum_i \omega_i(p_i\phi + r_i)}{\sum_i \omega_i}. \quad (1$$

The premise and consequent parameters are adjusted using backpropagation and Least Squares Estimation (LS [14], [15]

$$\begin{aligned} p_i(t+1) &= p_i(t) - \lambda\frac{\partial E}{\partial p_i} \\ r_i(t+1) &= r_i(t) - \lambda\frac{\partial E}{\partial r_i} \\ c_i(t+1) &= c_i(t) - \lambda\frac{\partial E}{\partial c_i} \\ a_i(t+1) &= a_i(t) - \lambda\frac{\partial E}{\partial a_i} \end{aligned} \quad (17)$$

being λ the learning rate.

IV. Proposed Solution

Due to the need of reducing the CM in DCO-OFDM scenarios, as explained in previous sections, the goal is to obtain a power derating reduction algorithm for DCO-OFDM signals in VLC. The key design premise is to get the best training set of data, and it is obtained with the RCM-ACE proposal in [12] because so far it proposes the algorithm that gets the largest CM reduction. The idea is to design an ANFIS that learns how to obtain DCO-OFDM signals with low crest factor from a flexible design.

A. Initial Analysis

In [12], a recent power derating algorithm for DCO-OFDM signals is proposed. It envisages our benchmark and allows us to select the best combination of the parameters V_{clip}, G and L in order to get the largest RCM reduction. These parameters are eligible in an ACE algorithm. V_{clip} represents the threshold to which the time-domain signal is clipped. G is called the extension gain, and is part of the clipping procedure of the ACE algorithm. Finally, L is necessary to guarantee a reasonable level of signal power, *i.e.*, it is the maximum value of the resulting real and imaginary components of the I/Q symbols.

An analysis of the RCM-ACE algorithm proposed in [12] has been carried out to obtain the best parameters. In the selection process of the V_{clip}, G and L parameters that better reduce the CM, it turned out that in 100 % of the cases, the saturation procedure was the least severe, that is, the optimal L parameter was always equal to the largest value in the allowed range ($L = [0.7, 1.4]$), *i.e.*, $L = 1.4$. However, the optimal V_{clip} and G parameters were variable. An increased L range up to the coherent value of 3 was also analysed and the result was that the optimal L parameter is 3 for a 100 % of DCO-OFDM symbols in a QPSK constellation. In the case of 16-QAM constellation, more than 95 % of symbols got this same maximum value as the optimal one. Thus, we can figure out that the larger the L parameter, the better CM reduction is obtained, but also the higher the signal energy is. It makes sense because larger values of L offer more flexibility and room to allocate the constellation points.

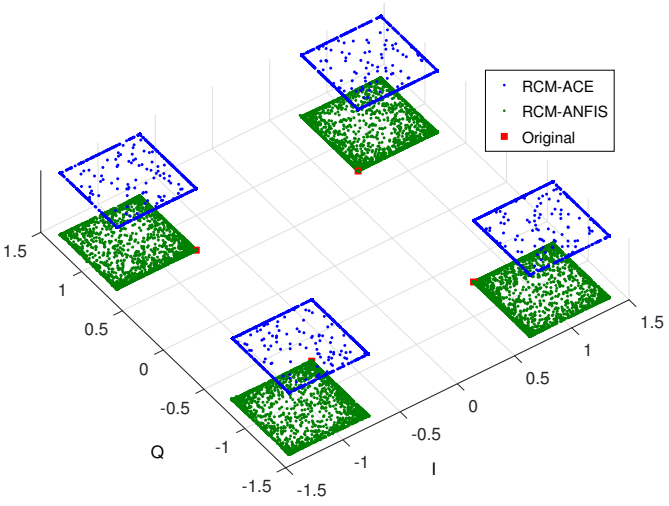

Fig. 5: Symbols distribution in RCM-ACE technique and RCM-ANFIS for a QPSK constellation.

These results provided an insight to design a flexible model based on ANFIS: the time-domain system is trained with RCM-ACE signals obtained with $L = 3$, and the following frequency-domain system with $L = 1.4$. The G and V_{clip} parameters are maintained in the range stated by [19]. In the time-domain system we get signals with very low CM but large mean energy. This mean energy will be reduced in the frequency-domain stage by limiting the L parameter to 1.4. It brings about a better distribution of symbols within the allowed regions, which are the squares formed from ±0.7 to ±1.4. This distribution can be observed in Fig. 5, where 100 OFDM symbols for a QPSK constellation and $N = 64$ subcarriers have been represented after using the RCM-ACE and the proposed RCM-ANFIS techniques. For the sake of clarity, the constellations have been drawn at various levels, that is, the third dimension is only for presentation purposes, and it has been included to distinguish the constellations obtained with the two different procedures. Also, the original constellation has been represented. The percentage of symbols that are moved into the proposed RCM-ANFIS is 56.9 %, whereas only a 27.3 % of symbols are moved in the RCM-ACE for a QPSK constellation.

B. ANFIS

There are two different ANFIS: the first one in the time domain, whose objective is to get time-domain signals with low RCM but with a relaxed restriction on signal energy (large value of L); the second one is a set of ANFIS in the frequency domain with the aim of learning the desired

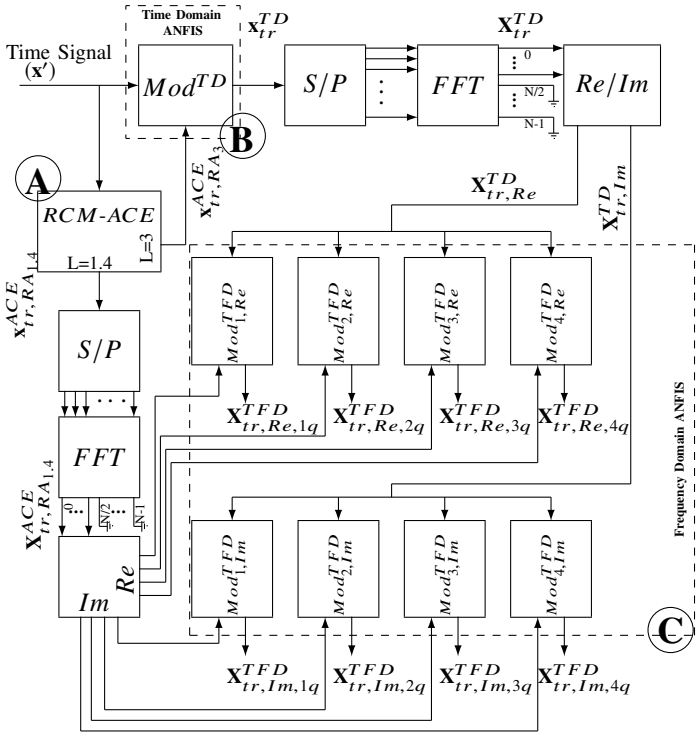

Fig. 6: Training scheme for Time-Domain model (Mod^{TD}) and Time-Frequency-Domain models (Mod^{TFD}_1, Mod^{TFD}_2, Mod^{TFD}_3, Mod^{TFD}_4) for real and imaginary parts.

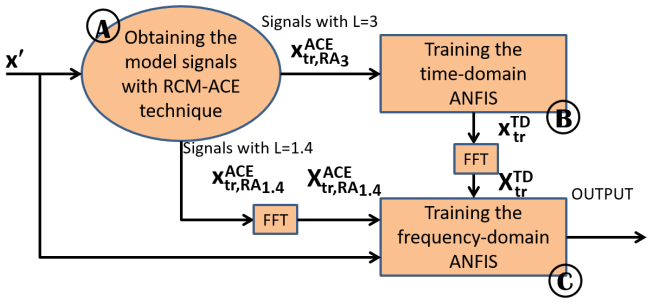

Fig. 7: Simplified diagram of the RCM-ANFIS training scheme.

constellation regions and thus, limiting the magnitude of the individual components (real and imaginary) so as to guarantee a reasonable level of signal energy (low value of L). Both use RCM-ACE signals to train the ANFIS. However, thanks to a combination of ANFIS schemes and a composition of RCM-ACE signals obtained with different parameters, the achieved performance is significantly better than the one resulting from the RCM-ACE proposal [12]. The training section can be observed in Fig. 6. Note that once the ANFIS are trained, they can work autonomously.

In the time-domain, signals are real so only one model is needed. In the frequency-domain, divisions into quadrants are carried out to simplify the training process. Each quadrant

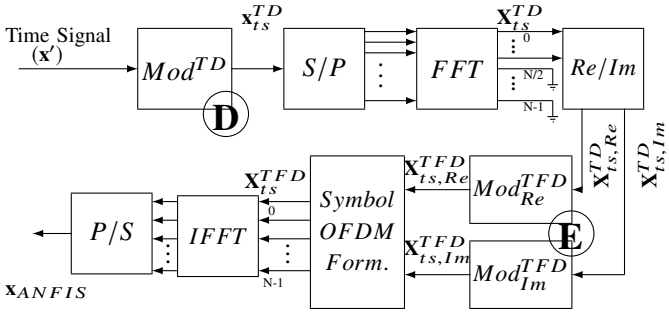

Fig. 8: Real-time scheme for Time-Domain model (Mod^{TD}) and Time-Frequency-Domain models (Mod^{TFD}_{Re}, Mod^{TFD}_{Im}) for each quadrant.

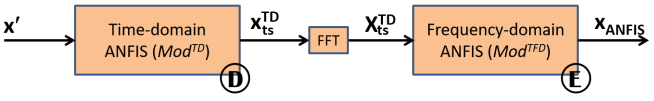

Fig. 9: Simplified diagram of the RCM-ANFIS real-time scheme.

needs two models because signals are complex and we only work with real values. Thus, 8 models are needed in the frequency domain and 9 as a whole.

Each ANFIS is trained with the fuzzy rules specified in Section III-A, but with different training signals. The training scheme is represented in detail in Fig. 6, and in a simplified way in Fig. 7. It is deployed to obtain the desired ANFIS set and make it ready to work in an autonomous way in the real-time scheme. This real-time scheme is depicted in Fig. 8 and in a simplified way in Fig. 9. For clarity purposes, Fig. 6-9 are labelled with letters from **A** to **E**.

On the one hand, in **B**, the first model (Mod^{TD}) learns in the time domain how the signals must be in order to have low power fluctuations but with no strict energy restriction (large L). To this purpose, it is trained with the signal from RCM-ACE algorithm with $L = 3$ ($\mathbf{x}^{ACE}_{tr,RA_3}$). On the other hand, in **C**, the models in the frequency domain ($Mod^{TFD}_{1,Re}$, $Mod^{TFD}_{1,Im}$, $Mod^{TFD}_{2,Re}$, etc.) force the symbols to be within the correct regions and thus, we also use them for limiting energy consumption (low L). They use the signal from RCM-ACE algorithm with $L = 1.4$ ($\mathbf{x}^{ACE}_{tr,RA_{1.4}}$) to be trained.

The procedure is as follows:

1) **Obtaining the training signals for the model** (label **A** in Fig. 6 and Fig. 7): The time-domain original DCO-OFDM signal ($\mathbf{x}'$) is used as the input for the RCM-ACE module to reduce signal fluctuations according to the RCM-ACE scheme [12]. The resulting signals are $\mathbf{x}^{ACE}_{tr,RA_3}$ and $\mathbf{x}^{ACE}_{tr,RA_{1.4}}$. These are the model signals that we want to obtain with ANFIS once they are trained. $\mathbf{x}^{ACE}_{tr,RA_3}$ is obtained with $L = 3$ and $\mathbf{x}^{ACE}_{tr,RA_{1.4}}$ with $L = 1.4$. The clipping threshold V_{clip} and the extension gain G are variable but maintained in the range mentioned in [19].

2) **Training the time-domain ANFIS (Mod$^{\mathbf{TD}}$)** (label **B** in Fig. 6 and Fig. 7): Signal $\mathbf{x}_{tr}^{TD}$ is obtained after the $ANFIS\ Mod^{TD}$ trained with $\mathbf{x}_{tr,RA_3}^{ACE}$ and $\mathbf{x}'$. The original $\mathbf{x}'$ specifies the kinds of signals that the $ANFIS$ will receive, whereas $\mathbf{x}_{tr,RA_3}^{ACE}$ means the objective signal. Both are used to compute the premise and consequent parameters and to make the $ANFIS$ trained. Signal $\mathbf{x}_{tr}^{TD}$ will be used as an input to train the frequency-domain models. Note that $\mathbf{X}_{tr}^{TD}$ is formed by only the first half of the subcarriers because the second one is just its Hermitian symmetry.
3) **Training the 8 frequency-domain ANFIS (Mod$^{\mathbf{TFD}}$)** (label **C** in Fig. 6 and Fig. 7): Once the symbol DCO-OFDM ($\mathbf{X}_{tr,RA_{1.4}}^{ACE}$) is obtained by a FFT operation, it is separated in the four quadrants as well as in real and imaginary parts. In that way, there are 8 simple frequency-domain models that can be easily trained: $Mod_{1,Re}^{TFD}$, $Mod_{1,Im}^{TFD}$, $Mod_{2,Re}^{TFD}$, $Mod_{2,Im}^{TFD}$, $Mod_{3,Re}^{TFD}$, $Mod_{3,Im}^{TFD}$, $Mod_{4,Re}^{TFD}$, $Mod_{4,Im}^{TFD}$. These frequency-domain models are trained with $\mathbf{X}_{tr,RA_{1.4}}^{ACE}$ and $\mathbf{X}_{tr}^{TD}$, after classifying the symbols in 4 quadrants and dividing them in real and imaginary parts. Note that the half of symbols of $\mathbf{X}_{tr}^{TD}$ are formed with the Hermitian symmetry and then discarded because they are repeated. $\mathbf{X}_{tr,RA_{1.4}}^{ACE}$ is the desired signal that is energetically restricted due to the value $L = 1.4$, whereas $\mathbf{X}_{tr}^{TD}$ is the input signal, *i.e.*, the kind of signal that will enter these modules.

Once the 9 ANFIS models are trained in an off-line way, we do not need to compute the RCM-ACE scheme ever again. The real-time phase is depicted in Fig. 8:

1) Time signal ($\mathbf{x}'$) passes through Mod^{TD}, and a signal with large energy but low RCM is obtained ($\mathbf{x}_{ts}^{TD}$) (label **D** in Fig. 8 and Fig. 9).
2) $\mathbf{X}_{ts,Re}^{TD}$ and $\mathbf{X}_{ts,Im}^{TD}$ signals result after a serial-to-parallel transformation, FFT operation, the rejection of the second half of subcarriers because they contain repeated symbols, and finally the separation of real and imaginary parts.
3) $\mathbf{X}_{ts,Re}^{TD}$ and $\mathbf{X}_{ts,Im}^{TD}$ are separated into 4 sets considering the 4 quadrants.
4) The signals are evaluated in the 8 frequency-domain models (only represented in Fig. 8 by Mod_{Re}^{TFD} and Mod_{Im}^{TFD}), obtaining $\mathbf{X}_{ts,Re}^{TFD}$ and $\mathbf{X}_{ts,Im}^{TFD}$ (label **E** in Fig. 8 and Fig. 9).
5) The symbol DCO-OFDM is formed by joining real and imaginary part, and the second half of subcarriers by means of a Hermitian symmetry.
6) $\mathbf{x}_{ANFIS}$ is obtained after an IFFT operation and a parallel-to-serial conversion. It is a signal with derated power and low RCM, energetically restricted ($L = 1.4$) and whose frequency-domain symbols are not in prohibited regions (See Fig. 5).

For the training phase, 10000 DCO-OFDM symbols and 10 (2) Gaussian input membership functions have been carried out in the time-domain (frequency-domain) ANFIS.

TABLE I: Complexity summary

	RCM-ACE	**Proposed RCM-ANFIS**
Additions of real values	40 x N	28 x N - 12
Multiplications of real values	42 x N	60 x N - 20
Additions of complex values	2 x N	0
Multiplications of complex values	N	0
Check operations	6 x N	0
(I)FFT	2	2

C. Complexity Analysis

Once the training was carried out off-line, the operational performance of the system is as simple as introducing the input signal, and obtaining the output after computing some additions and multiplications of real values. Concretely, the number of additions and multiplications in our proposal is 28 x N - 12 and 60 x N - 20, respectively, being N the number of subcarriers. These numbers result from equations (12)-(16), and the real-time scheme in Fig. 8. Since these numbers can change depending on the programming language, a more reliable metric is asymptotic behaviour. This is a linear algorithm $O(N)$ because it is just based on additions and multiplications without any loop and more complex operations. Table I presents a comparison in number of the operations between RCM-ACE and RCM-ANFIS algorithms. Note that, although our proposal RCM-ANFIS needs a lower number of operations, both have the same asymptotic behaviour $O(N)$ and as a result, computational time is similar.

V. Results

The performance of the proposal is evaluated by means of Monte Carlo simulations in a scenario where the used white LED is a Golden Dragon LA W57B [20]. Its transfer function is analytically described in [21]. As it has been mentioned, the ANFIS scheme is only necessary on the transmitter side, being completely transparent on the receiver side (see Fig. 1). The reason is that we always distort the symbols within the allowable regions, which involves not decreasing the minimum distance between symbols and thus, the performance of the maximum likelihood decoding algorithm is not modified. The system is assessed for N equal to 64, 256 and 1024 subcarriers, QPSK and 16-QAM constellations.

The Complementary Cumulative Distribution Function (CCDF) is used to show the results. Fig. 10 and Fig. 11 show the probability that the RCM metric is higher than a certain value denoted as RCM_0 for QPSK and 16-QAM constellations, respectively. The CCDF curves are obtained with the simulation of 10^5 random DCO-OFDM symbols. In order to simulate a real analogue signal, an oversampling factor of 4 is used [22]. For each number of subcarriers, three different curves are plotted: CCDF without PAPR/CM reduction, RCM-ACE method and the proposed RCM-ANFIS method. For the sake of clarity, results obtained by the traditional ACE algorithm are not plotted [12]. For each N and constellation order, a notable reduction is observed in RCM at CCDF = 10^{-4}. Table II summarizes the RCM reductions at CCDF = 10^{-4} for the RCM-ACE and RCM-ANFIS, with respect to the CCDF curve of the signal with no reduction.

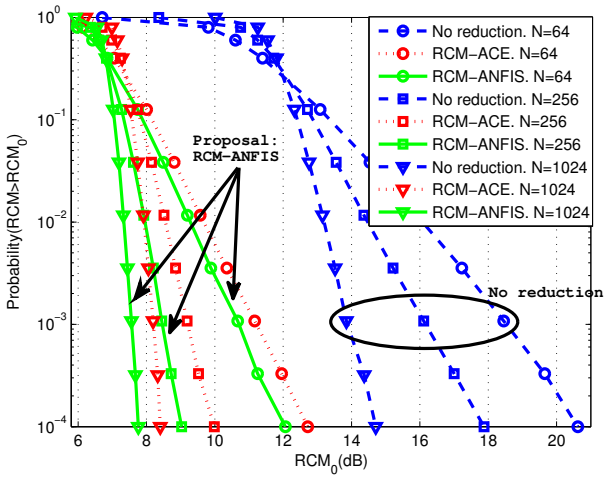

Fig. 10: CCDF of RCM of a DCO-OFDM signal for a QPSK constellation.

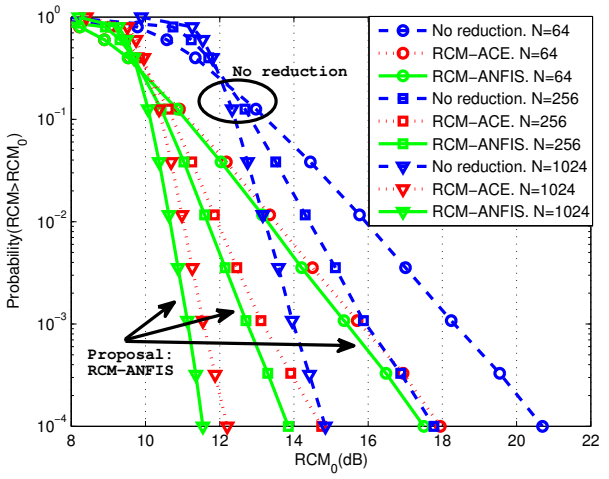

Fig. 11: CCDF of RCM a DCO-OFDM signal for a 16-QAM constellation.

TABLE II: RCM Reductions @ $CCDF = 10^{-4}$

Constellation	Method	$N = 64$	$N = 256$	$N = 1024$
QPSK	RCM-ACE	7.9 dB	7.8 dB	6.3 dB
	RCM-ANFIS (proposal)	8.6 dB	8.9 dB	7.0 dB
16-QAM	RCM-ACE	2.7 dB	3.0 dB	2.5 dB
	RCM-ANFIS (proposal)	3.2 dB	3.9 dB	3.3 dB

These reductions correspond to an improvement of EVM, ICE and BER analyzed in next subsections. The RCM reduction gets lowered at N=1024 because a fixed configuration of membership functions was employed in order to limit the complexity.

A. Energy Consumption

A biasing level is necessary in order to illuminate the room in DCO-OFDM systems for VLC. However, energy consumption is as important as in any communication system. Fig. 5 represents the symbol distribution in a QPSK constellation

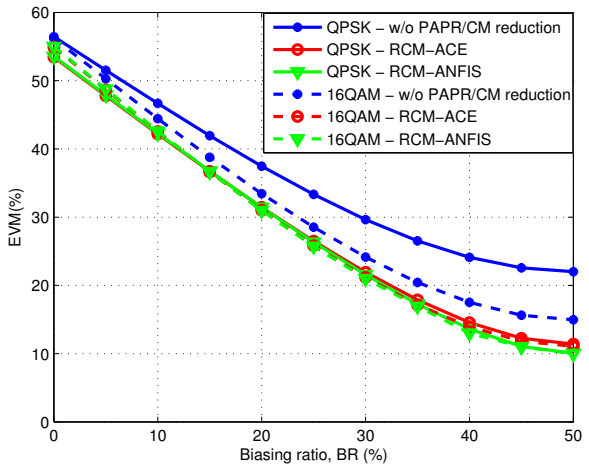

Fig. 12: EVM versus biasing ratio for QPSK and 16-QAM constellations with an IBO of 8.9dB and 10.4dB, respectively.

for RCM-ACE and RCM-ANFIS methods. Note that there is an energy increase with respect to the original constellation, in exchange for a better performance in the general system thanks to a RCM reduction. However, it corresponds only to an increase of approximately 1 % of the total energy consumption, which is almost insignificant.

B. EVM Analysis

Signal distortions are evaluated by means of the EVM (eq. (8)). In Fig. 12, the curves of EVM versus BR for an IBO of 8.9 dB (10.4 dB) in a QPSK (16-QAM) constellation are shown. This IBO value offers an EVM of 10 % for our proposal when BR is 50 %. Six different curves are represented: without PAPR/CM reduction, with the RCM-ACE technique introduced in [12] and the proposed RCM-ANFIS method, for QPSK and 16-QAM constellations. As it can be seen, our proposal reduces the EVM with respect to the result when no PAPR/CM reduction technique is applied. For a QPSK constellation and a BR equals to 50 %, an EVM of 22 % is obtained with no PAPR/CM reduction technique, whereas an EVM of 10 % results with the RCM-ANFIS method. Besides, it outperforms the results obtained with the RCM-ACE technique, an EVM of 12 % for a BR equals to 50 %. Improvements are also achieved when a 16-QAM constellation is employed. Note that EVM results for a 16-QAM constellation are better than for QPSK, both without PAPR/CM reduction, due to having a larger IBO value for a 16-QAM constellation which makes avoid largely the clipping effect.

Table III contains the different IBO values and gains resulting from applying the different techniques achieving EVM=10 %, 15 % and 20 %. Note that a gain of up to 2.8 dB is achieved with our proposed method, and it overcomes the RCM-ACE technique by up to 0.3 dB for QPSK and 0.2 dB for a 16-QAM constellation and EVM=10 %. Similar results have been obtained for $N = \{64, 256, 1024\}$.

TABLE III: IBO Values and IBO Gain

Constellation	Method	EVM = 10%		EVM = 15%		EVM = 20%	
		IBO (dB)	IBO gain (dB)	IBO (dB)	IBO gain (dB)	IBO (dB)	IBO gain (dB)
QPSK	without PAPR/CM reduction	11.7	-	10.4	-	9.3	-
	RCM-ACE	9.2	2.5	8.1	2.3	7.2	2.1
	RCM-ANFIS (proposal)	8.9	2.8	7.9	2.5	7	2.3
16-QAM	without PAPR/CM reduction	11.7	-	10.4	-	9.3	-
	RCM-ACE	10.6	1.1	9.5	0.9	8.5	0.8
	RCM-ANFIS (proposal)	10.4	1.3	9.3	1.1	8.3	1.0

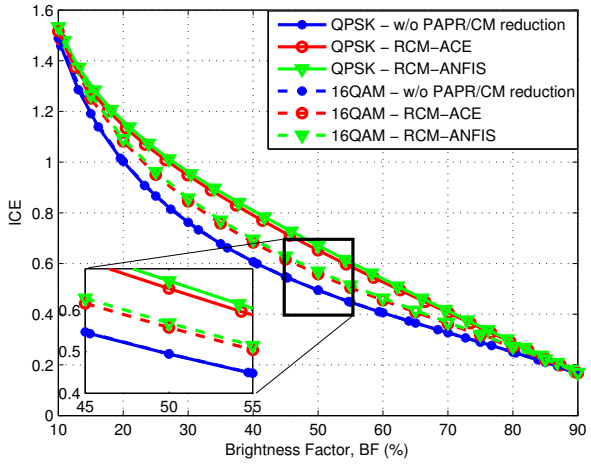

Fig. 13: ICE versus Brightness Factor for EVM = 10 % with QPSK and 16-QAM constellations.

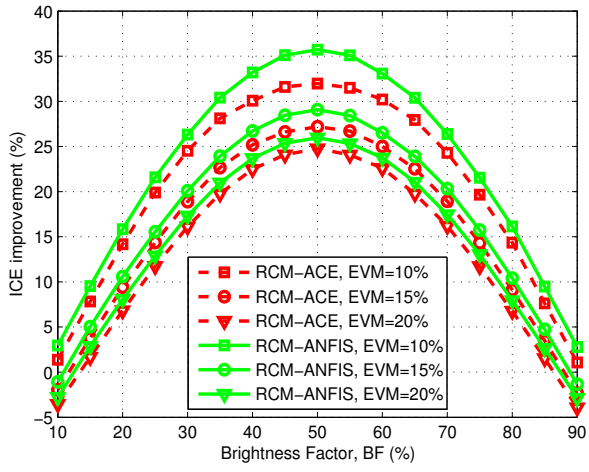

Fig. 14: ICE improvement versus Brightness Factor for EVM = {10 %, 15 %, 20 %} and QPSK constellation.

C. Illumination-to-Communication Conversion Efficiency Analysis

The VLC system efficiency is evaluated by means of the ICE (eq. (9)) [18]. The results are depicted in Fig. 13, where an improvement regardless the BF is achieved with the proposed RCM-ANFIS over the signal without PAPR/CM reduction technique. It also overcomes the RCM-ACE technique. To obtain these curves, the IBO is configured such that it provides an EVM=10 %.

Fig. 14 and Fig. 15 contain the curves of ICE improvement with respect to the signal without reduction technique, for QPSK and 16-QAM constellations, respectively, and different values of EVM. Note that an improvement is achieved in the whole BF range comparing to the RCM-ACE technique, but the highest improvement is achieved when the BF is equal to 50 %.

Table IV shows the ICE gains extracted from the Fig. 14 and Fig. 15. The improvement of our proposal with respect to the RCM-ACE technique is also included. A maximum ICE gain of 35.8 % is achieved with RCM-ANFIS for a QPSK constellation, and an improvement of up to 3.9 % with respect to the RCM-ACE technique is also obtained. The proposed method improves up to a 15 % the original signal for 16-QAM constellation, and a maximum gain of up to 2.3 % is achieved compared to the RCM-ACE technique. Similar results have been obtained for $N = \{64, 256, 1024\}$.

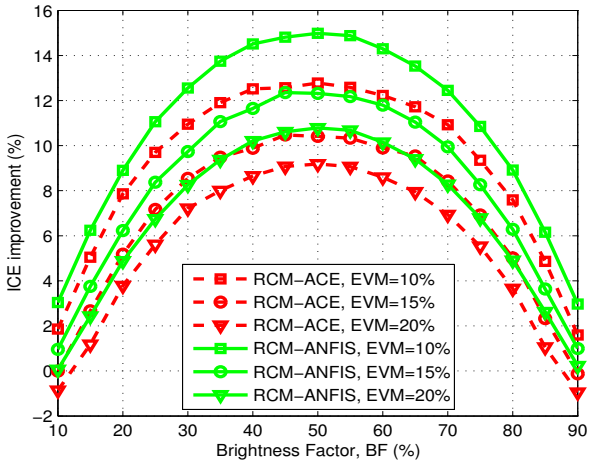

Fig. 15: ICE improvement versus Brightness Factor for EVM = {10 %, 15 %, 20 %} and 16-QAM constellation.

D. BER Analysis

Fig. 16 depicts the BER analysis of this approach and a comparison with the other techniques. These curves are obtained with a BR of 50 % and an IBO so that the EVM is equal to 10 %. Note that most of the curves suffer an error floor due to the clipping effect. It does not allow decreasing

TABLE IV: ICE Gain Measured at BF = 0.5

Constellation	Method	EVM = 10%		EVM = 15%		EVM = 20%	
		ICE Gain (%)	Improvement (%)	ICE Gain (%)	Improvement (%)	ICE Gain (%)	Improvement (%)
QPSK	RCM-ACE	31.9	-	27.1	-	24.7	-
	RCM-ANFIS (proposal)	35.8	3.9	29.1	2.0	26.0	1.3
16-QAM	RCM-ACE	12.7	-	10.4	-	9.1	-
	RCM-ANFIS (proposal)	15.0	2.3	12.4	2.0	10.8	1.7

the BER more. This aspect indeed validates the research in new methods for PAPR/CM reduction, and then, this proposal. These curves may be different if another LED model is used.

The proposed RCM-ANFIS reduces the BER in comparison to the RCM-ACE technique and the signal without reduction technique. Both in QPSK and 16-QAM, signals without reduction technique suffer a saturation and have a noise floor in $4 \cdot 10^{-3}$ and 10^{-3}, respectively. It makes clear the need of a CM reduction technique giving a much better BER performance as a result. Results of RCM-ANFIS in QPSK are better than in 16-QAM because the minimum distance between I/Q symbols in QPSK is larger and also has a larger percentage of points to be moved in the constellation: 100 % in QPSK whereas 75 % in 16-QAM. Interior I/Q symbols in a 16-QAM constellation cannot be moved in order not to decrease the minimum distance between symbols and then increase the BER.

Note that these performance differences will be larger if another LED model with a less linear transfer function and smaller dynamic range is used.

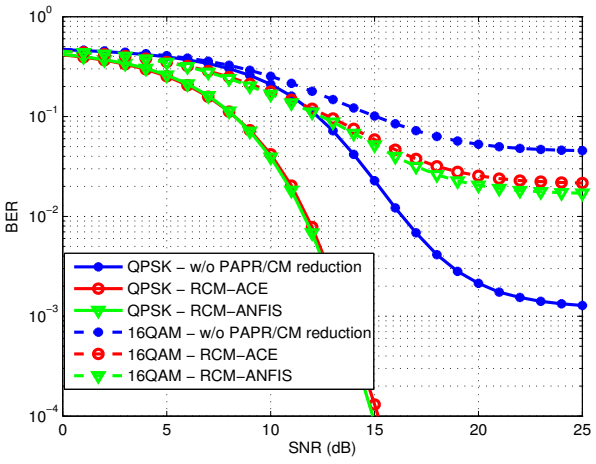

Fig. 16: BER versus SNR for EVM = 10 % with QPSK and 16-QAM constellations.

VI. Conclusion

This paper presents an efficient technique for power derating DCO-OFDM signals based on ANFIS. Using a proper combination of optimized training models, the RCM-ANFIS obtains efficient power derated DCO-OFDM signals. Once trained, the ANFIS models can work autonomously. RCM metric is chosen to build a more effective algorithm, achieving a reduction of 8.9 dB with respect to the original DCO-OFDM signal at $CCDF = 10^{-4}$, unlike the 7.8 dB reduction obtained by the RCM-ACE method. Since the clipping effect is mitigated due to this power derating technique, the signal degradation is reduced 12 % in EVM at the most for a fixed IBO value. On fixing an EVM value, the RCM-ANFIS technique overcomes the RCM-ACE technique and achieves IBO gains of 2.8 dB (for EVM = 10 %). It produces ICE gains above 35 %, leading to improvements of up to 3.9 % with respect to the RCM-ACE method. Finally, improvements in BER are also obtained. For all the studied parameters and figures of merit, the implementation of this technique in a DCO-OFDM VLC system involves a better efficiency between the communication capacity and the illumination level.

Acknowledgment

This work has been partly funded by the Spanish MECD FPU fellowship program, granted to Borja Genovés Guzmán, and the Spanish national projects 'GRE3N-SYST' (id. TEC2011-29006-C03-03) and 'ELISA' (id. TEC2014-59255-C3-3-R). The authors would like to thank José García Doblado because of his orientation at the beginning of the work.

References

[1] C. Liu, J. Wang, L. Cheng, M. Zhu, and G.-K. Chang, "Key Microwave-Photonics Technologies for Next-Generation Cloud-Based Radio Access Networks," *J. Lightw. Technol.*, vol. 32, no. 20, pp. 3452–3460, Oct 2014.

[2] Y.-N. R. Li, J. Li, W. Li, Y. Xue, and H. Wu, "CoMP and Interference Coordination in Heterogeneous Network for LTE-Advanced," in *Proc. IEEE Globecom Workshops*, 2012, pp. 1107–1111.

[3] Li-Fi Consortium. [Online]. Available: http://www.lificonsortium.org/

[4] *IEEE Standard for Local and Metropolitan Area Networks–Part 15.7: Short-Range Wireless Optical Communication Using Visible Light*, IEEE Std. 802.15.7, 2011.

[5] B. Genoves Guzman, A. Lancho Serrano, and V. P. Gil Jimenez, "Cooperative Optical Wireless Transmission for Improving Performance in Indoor Scenarios for Visible Light Communications," *IEEE Trans. Consum. Electron.*, vol. 61, no. 4, pp. 393–401, November 2015.

[6] J. Carruthers and J. Kahn, "Multiple-Subcarrier Modulation for Nondirected Wireless Infrared Communication," *IEEE J. Sel. Areas Commun.*, vol. 14, no. 3, pp. 538–546, April 1996.

[7] J. Armstrong and A. Lowery, "Power efficient optical OFDM," *Electron. Lett.*, vol. 42, no. 6, pp. 370–372, March 2006.

[8] N. Fernando, Y. Hong, and E. Viterbo, "Flip-OFDM for Unipolar Communication Systems," *IEEE Trans. Commun.*, vol. 60, no. 12, pp. 3726–3733, December 2012.

[9] S. D. Dissanayake and J. Armstrong, "Comparison of ACO-OFDM, DCO-OFDM and ADO-OFDM in IM/DD Systems," *J. Lightw. Technol.*, vol. 31, no. 7, pp. 1063–1072, April 2013.

[10] S. H. Han and J. H. Lee, "An Overview of Peak-To-Average Power Ratio Reduction Techniques for Multicarrier Transmission," *IEEE Wireless Commun.*, vol. 12, no. 2, pp. 56–65, April 2005.
[11] TDoc R1-060023, "Cubic Metric in 3GPP-LTE," *3GPP TSG RAN WG1, Tech. Rep.*, 2006.
[12] J. Garcia Doblado, A. Cinta Oria Oria, V. Baena-Lecuyer, P. Lopez, and D. Perez-Calderon, "Cubic Metric Reduction for DCO-OFDM Visible Light Communication Systems," *J. Lightw. Technol.*, vol. 33, no. 10, pp. 1971–1978, May 2015.
[13] J.-S. Jang, "ANFIS: Adaptive-Network-based Fuzzy Inference System," *IEEE Trans. Syst., Man, Cybern.*, vol. 23, no. 3, pp. 665–685, May 1993.
[14] V. P. Gil Jimenez, Y. Jabrane, A. Garcia Armada, B. A. E. Said, and A. A. Ouahman, "Reduction of the Envelope Fluctuations of Multi-Carrier Modulations using Adaptive Neural Fuzzy Inference Systems," *IEEE Trans. Commun.*, vol. 59, no. 1, pp. 19–25, January 2011.
[15] L. Aik, S. Yogan, and O. Jayakumar, "A Study of Neuro-Fuzzy System in Approximation-based Problems," *MATEMATIKA*, vol. 23, no. 2, pp. 113–130, 2008.
[16] Y. Jabrane, V. P. G. Jimenez, A. G. Armada, B. A. E. Said, and A. A. Ouhman, "Evaluation of the effects of pilots on the envelope fluctuations reduction based on neural fuzzy systems," in *2010 IEEE 11th International Workshop on Signal Processing Advances in Wireless Communications (SPAWC)*, June 2010, pp. 1–5.
[17] Z. Yu, "Optical Wireless Communications with Optical Power and Dynamic Range Constraints," *Ph.D. dissertation, Dept. Elect. and Comp. Eng., Georgia Inst. Tech., Atlanta, GA, USA*, May 2014.
[18] Z. Yu, R. J. Baxley, and G. T. Zhou, "Peak-to-average power ratio and illumination-to-communication efficiency considerations in visible light OFDM systems," in *2013 IEEE International Conference on Acoustics, Speech and Signal Processing*, May 2013, pp. 5397–5401.
[19] European Telecommunications Standards Institute, "Digital Video Broadcasting (DVB); Frame Structure Channel Coding and Modulation for a Second Generation Digital Terrestrial Television Broadcasting System (DVB-T2)," *ETSI EN 302 755*, vol. 1.3.1, April 2012.
[20] "Golden Dragon LA W57B Datasheet," *OSRAM Opto Semiconductors GmbH*, May 2003.
[21] H. Elgala, R. Mesleh, and H. Haas, "An LED Model for Intensity-Modulated Optical Communication Systems," *IEEE Photon. Technol. Lett.*, vol. 22, no. 11, pp. 835–837, June 2010.
[22] J. Tellado, "Multicarrier Modulation With Low PAR: Applications to DSL and Wireless," *New York, NY, USA: Springer*, 2000.

Borja Genovés Guzmán (S'14) received his B.Sc. and double M.Sc. degrees in electrical engineering from the University Carlos III of Madrid and the Institut Mines-Télécom, France, in 2013 and 2015, respectively, both with honours. He received the First prize in Graduation National Awards by the Ministry of Education, Culture and Sports of Spain. He is currently a Ph.D. candidate in the Communications Research Group at the University Carlos III of Madrid. He is a recipient of an FPU scholarship from the Spanish Ministry of Education, Culture and Sports of Spain. His current research focuses on new techniques to improve the efficiency of optical wireless communications systems.

PLACE
PHOTO
HERE

Víctor P. Gil Jiménez Biography text here.